scientific reports

Check for updates

OPEN

Astaxanthin mitigates cardiac toxicity induced via doxorubicin by alleviating mitochondrial fission and autophagy in rats

Yongjing He[1,6], Dan Wu[2,6], Qianqian Wu[1], Sisi Huang[3], Yuansheng Zhan[3], Jiaqiang Deng[3], Jing yu Chen[4], Lu xie[1]✉ & Junhui Zheng[3,5]✉

Doxorubicin (DOX)-induced cardiotoxicity is the most prevalent adverse reaction of DOX during chemotherapy and significantly impacts its clinical application. At present, clinical interventions for mitigating DOX-induced cardiotoxicity remain sub-optimal. Mitochondria are the primary target organ of DOX-induced cardiotoxicity, which can result in cardiac mitochondrial dynamic imbalance and impaired mitochondrial autophagy. Astaxanthin (ASTA) is an antioxidant that exerts cardioprotective effects in various cardiac diseases. Meanwhile, it can also ameliorate mitochondrial dynamic dysregulation and suppress the abnormal activation of autophagy. Therefore, ASTA was administered to a rat model of DOX-induced cardiotoxicity, and its cardioprotective effects were observed. Additionally, the mechanisms underlying its cardioprotective effects were investigated by detecting proteins related to mitochondrial dynamics and mitophagy. The results revealed that ASTA up-regulated the expression of mitochondrial fusion protein 2(Mfn2) and Optic Atrophy 1(OPA1), reduced the expression level of dynamin-related protein 1 (Drp1) and Fission 1 Protein(Fis-1), and regulated PTEN-Induced Putative Kinase 1(PINK1)/ Parkin RBR E3 Ubiquitin Protein Ligase (Parkin)-mediated mitochondrial autophagy to alleviate mitochondrial damage in the rat model. Consequently, we hypothesize that ASTA alleviates DOX-induced cardiotoxicity by regulating mitochondrial dynamic imbalance and mitophagy, thereby attenuating mitochondrial damage and exerting cardioprotective effects. Overall, these findings indicate that ASTA holds promise as a prospective drug for ameliorating DOX-induced cardiotoxicity.

Keywords Astaxanthin, Doxorubicin, Cardiotoxicity, Mitochondrial dynamics, Mitochondria autophagy

As is well documented, the anthracycline chemotherapy drug doxorubicin (DOX) has been extensively utilized for the treatment of diverse malignancies[1]. However, despite its potent efficacy, up to 25% of patients experience DOX-induced cardiac injury[2]thereby imposing limitations on its utilization. Notably, DOX-induced cardiac injury is dose-dependent and characterized by reduced left ventricular ejection fraction, increased ventricular wall thickness, arrhythmia, heart failure, and mortality[3]. Although DOX-induced cardiac injury is well known, there is no effective treatment other than routine adjustment of DOX dose[4]. Currently, Dexrazoxane is the only FDA-approved protective agent for the treatment of DOX-induced cardiac injury[5]. However, an earlier study reported that the co-administration of dexrazoxane could potentially modulate the reactivity of DOX towards tumors and consequently elevate the susceptibility to secondary malignancies, thereby significantly impacting its clinical utility[6]. Therefore, there is an urgent need to develop highly effective and safe complementary interventions without adversely impacting the anti-tumor efficacy of doxorubicin, aiming to prevent adverse cardiac events in cancer chemotherapy survivors.

The pathogenesis underlying DOX-induced cardiac injury involves multiple mechanisms, with oxidative stress being one of the major contributors[7,8]. Numerous studies have established the role of mitochondria as a

[1]Department of Physiology, Pre-Clinical Science, Guangxi Medical University, Nanning 530021, Guangxi, China. [2]Department of Intensive Care Unit, Guangxi Medical University Cancer Hospital, Nanning 530021, Guangxi, China. [3]Department of Cardiovascular Medicine, Guangxi Medical University Cancer Hospital, Nanning 530021, Guangxi, China. [4]Department of Endocrinology, Guangxi Medical University Cancer Hospital, Nanning 530021, Guangxi, China. [5]State Key Laboratory of Targeting Oncology, Guangxi Medical University, Nanning 530021, Guangxi, China. [6]Yongjing He and Dan Wu contributed equally to this work. ✉email: xielu8282@163.com; 13207811035@163.com

source and target of oxidative stress[9–11]. Meanwhile, mitochondria are considered the primary organelles affected by DOX, with mitochondrial dysfunction also serving as a significant indicator of its cardiotoxic effects[12]. Of note, mitochondria continuously undergo fusion and fission, collectively termed mitochondrial dynamics[13]. Mitochondrial fusion has been described as a defensive response to enhance resistance to stress. In contrast, mitochondrial fission not only supports the high energy demands of cardiomyocytes but also allows the removal of dysfunctional mitochondrial fractions from the mitochondrial network to preserve mitochondrial integrity[13]. Excessive mitochondrial division or lysis can trigger cell apoptosis and necrosis, resulting in the deterioration of cardiac function[14]. Dysregulation of mitochondrial dynamics is a hallmark of DOX-induced cardiac injury[13,15–17]. Specifically, DOX disrupts mitochondrial dynamics by promoting mitochondrial fission and suppressing mitochondrial fusion. A recent study reported that mitochondrial fusion 2 (Mfn2) overexpression restored mitochondrial fusion and attenuated DOX-induced apoptosis, oxidative stress, and cardiac dysfunction[18]. At the same time, mitochondrial fission protein dynamin-related protein 1 (Drp1) heterozygous knockout has been shown to protect against DOX-induced cardiotoxicity[19]. Therefore, inhibiting fission or promoting fusion may assist in mitigating DOX-induced cardiac injury.

DOX-induced cardiac mitochondrial toxicity induces autophagic (including mitochondrial autophagy) responses[20]. While moderate levels of mitochondrial autophagy contribute to the maintenance of physiological cellular autophagy by eliminating damaged mitochondria, excessive activation severely impairs mitochondrial function[21,22]. In cellular models of DOX-induced autophagic overstimulation, cardiac protection was achieved using inhibitors of autophagy initiation[20,23–25]. Therefore, the targeted modulation of mitochondrial autophagy may present a promising therapeutic approach for the management of DOX-induced cardiac injury.

Astaxanthin (ASTA), a member of the carotenoid family, has garnered significant attention owing to its potent antioxidant properties[26]. ASTA has been investigated in the treatment research of various heart diseases such such as heart failure[27] and ischemic cardiomyopathy[28]. Previous studies concluded that ASTA can enhance cardiac function by attenuating oxidative stress damage and mitochondrial swelling, thereby exerting cardioprotective effects. Moreover, ASTA can enhance mitochondrial function through the activation of the Nuclear factor (erythroid-derived 2)-like 2(Nrf2)/ Heme Oxygenase-1(HO-1)pathway, thereby promoting autophagy and concurrently inhibiting ferroptosis[29]. Furthermore, it can alleviate the imbalance of mitochondrial dynamics, inhibit mitochondrial fission, and promote mitochondrial fusion[30,31]. A study had shown that ASTA alleviated oxidative stress and DOX-induced apoptosis and related cardiac development abnormalities in zebrafish embryos[32]. However, the effects of ASTA on cardiac mitochondria following the administration of doxorubicin, mitochondrial dynamics, and autophagy remain elusive.

Based on the aforementioned evidence, we postulate that ASTA can mitigate the imbalance in mitochondrial fusion and fission and suppress DOX-induced mitophagy, thereby exerting cardioprotective effects. A pooled analysis involving 630 patients with breast cancer and lung cancer demonstrated that the incidences of congestive heart failure were 4.7%, 26%, and 48% when the cumulative dose of doxorubicin reached 400, 550, and 700 mg/m^2, respectively[33]. In order to guarantee the success rate of animal modeling, we selected the dose of doxorubicin as 15 mg/kg, which is equivalent to 800 mg/m2 for a 70 kg man. Furthermore, previous studies have demonstrated that significant cardiotoxicity occurs in rats when the cumulative dose reaches 15 mg/kg[34]. Therefore, a rat model of DOX-induced cardiac injury was established to explore the effects of ASTA on DOX-induced cardiac mitochondrial damage, mitochondrial dynamics, and autophagy.

Methods

Animals and treatments

Healthy male rats (6–8 weeks old) were sourced from the Laboratory Animal Center of Guangxi Medical University. All experiments were conducted in accordance with the Guidelines on the Care and Use of Laboratory Animals established by the National Institutes of Health. This study was approved by the Animal Welfare and Ethics Committee of Guangxi Medical University (approval number: 202404007). Prior to the experiments, the rats were housed in a controlled environment with a 12-hour light/dark cycle and ad libitum access to food and water for one week. Afterward, the rats were randomly assigned to four groups, namely the sham group, DOX group, DOX + ASTA (25 mg/kg) group, and DOX + ASTA (50 mg/kg) group. The rats in the DOX group received intraperitoneal injections of doxorubicinat a dose of 3 mg/kg once every 3 days for a total of five times, the vehicle was prepared in saline with a final volume of 0.5 mL[35]. The Rat in the treatment group received the same treatment as the DOX group, but on top of that, ASTA was administered orally via intragastric administration 30 min later, at a dose of 25 mg/kg/day or 50 mg/kg/day for 15 consecutive days[36,37],Astaxanthin was dissolved in olive oil with a final volume of 1 mL. Rats in the Sham group received saline via intraperitoneal injection at the same volume and frequency as the DOX group, and were administered olive oil by oral gavage matching the volume and frequency of the ASTA (25 mg/kg) group, and ASTA (50 mg/kg) group. Doxorubicin (CSNPHARM, CSN16255, China) and Astaxanthin (CSNPHARM, CSN20493, China) were both acquired from CSNPHARM Company. Each experimental group consisted of at least six rats, and all necessary measures were taken to minimize animal suffering throughout the experiments. After the completion of the experiment, rats were anesthetized and sacrificed by using an excessive dose of pentobarbital sodium for subsequent experiments.

Echocardiography

At the end of the 15-day dosing regimen, cardiac function was assessed using ultra-high-resolution echocardiography. The rats were mildly anesthetized via inhalation of 1.5% isoflurane (RWD, R510-22-10, China) and subsequently placed on a heating table to maintain normal body temperature. A digital animal ultrasound imaging system (Esaote, Italy) equipped with a 12 MHz probe was employed for cardiac imaging. Two-dimensional echocardiography and M-mode echocardiographic assessments were performed in the parasternal long-axis view, and ejection fraction (EF) and fractional shortening (FS) were calculated.

ELISA assay

At the 16th day of the study, after performing ultrasonic measurements, blood samples were collected from each rat via arterial catheterization into syringes and subsequently placed at room temperature for two hours. Following this, the samples were centrifuged at 4℃ and 3000 RPM using a high-speed centrifuge for 10 min. Next, the serum supernatant was extracted for further experimentation. The commercially available troponin I detection kit (NanJing JianCheng Bioengineering Institute, H149-1-1, China) was utilized to determine the concentration of troponin I in rat serum following the manufacturer's instructions.

Histological staining

The cardiac tissues of the rats were harvested on the 16th day of the study for histological staining .Fresh heart tissue samples were fixed in 4% paraformaldehyde at 4℃ overnight, following which they were embedded in paraffin and sectioned. The resulting sections were subsequently subjected to HE staining, and morphological changes in cardiomyocytes were visualized under a light microscope.

ATP content detection

The measurement of ATP was conducted using the colorimetric method. The principle is that creatine kinase catalyzes the reaction of adenosine triphosphate (ATP) and creatine to form phosphocreatine38. The amount of phosphorus generated was detected by the phosphomolybdate colorimetric method, and the ATP content was calculated accordingly.The specific steps were as follows: 50 mg of fresh myocardial tissue was taken and a 10% homogenate was made in pre-cooled pure water. After homogenization, the supernatant was collected and the protein concentration in the supernatant was simultaneously determined. According to the protocol provided by the ATP detection kit (Nanjing Jiancheng ATP detection kit, A095-1-1, China), blank tubes, standard tubes, measurement tubes, and control tubes were set up. 1 mmol/L ATP standard solution was added to the blank tube and control tube, and the collected supernatant was added to the measurement tube and control tube. 100 μl of final substrate solution I and 200 μl of substrate solution II were added to all tubes. 30 μl of pure water was added to the blank tube and control tube, while 30 μl of accelerator was added to the standard tube and measurement tube. The mixtures were mixed well and incubated at 37 °C for 30 min. After the water bath, 50 μl of precipitating agent was added to all tubes, mixed well, and centrifuged at 4000 rpm for 5 min. 300 μl of the supernatant from each tube was taken for measurement. 500 μl of chromogenic agent was added to the supernatant, mixed well, and left to stand at room temperature for 2 min. Finally, 500 μl of termination agent was added to all tubes, mixed well, and left to stand at 37 °C for 5–10 min. The absorbance values of each tube were measured at 636 nm with a light path of 0.5 cm using double distilled water as the blank. The final ATP content was calculated as: (A measurement - A control) / (A standard - A blank) × Concentration of the standard × sample dilution factor × protein concentration of the homogenate.

Ultrastructural assessment

The cardiac tissues of the rats were harvested on the 16th day of the study for transmission electron microscope Cardiac tissue samples were immersed in a vessel containing a fixative solution for electron microscopy. Thereafter, the tissue was meticulously dissected into 1 mm^3 fragments using a scalpel, followed by rinsing with PBS and immersion in fixative solution at room temperature for 24 h. The tissue samples were further fixed with 1% osmic acid. Afterward, the samples were dehydrated, embedded, and prepared into ultrathin sections. The slides were stained and observed under a transmission electron microscope (TEM). Images were captured and preserved for the ensuing analysis.

The specific implementation details of Flameng Score are as follows: Firstly, randomly select mitochondria from the electron microscopy images of each group, a total of 100 mitochondria. The average score of these 100 mitochondria represents the sample score. Next, calculate the average score of mitochondria for each sample. In brief, determine the mitochondrial score for each sample to be a score ranging from 0 to 4, with higher scores indicating more severe damage. The specific scoring rules are detailed in Appendix 1.

Western blot analysis

The cardiac tissues of the rats were harvested on the 16th day of the study for Western blot experiments. Heart tissue samples were homogenized in cold RIPA tissue lysate (Solarbio, P0010, China) supplemented with PMSF protease inhibitor (Solarbio, P0100, China) and phosphatase inhibitor (Solarbio, P1260, Chian) for 10 min. Total proteins were obtained by high-speed centrifugation. Protein concentrations were quantified using the BCA assay (Boeter, AR0146, China). Next, 30 μg of protein was loaded onto a 10% or 12% w/v sulfate-polyacrylamide gel for electrophoresis (SDS-PAGE) for 2 h. Subsequently, the proteins were transferred to a polyvinylidene fluoride (PVDF) membrane (Millipore Corp, Billerica, MA). The membrane was washed three times with Tris-buffered saline containing Tween 20 (TBST) for 10 min each time. Subsequently, the membrane was incubated with primary antibodies, including DRP1 resistant (1:1000, Cell Signaling Technology, #5391), Mfn2(1:1000, Cell Signaling Technology,# 9482T), LC3 (1:1000, Cell Signaling Technology,#12741T), p62 (1:1000, Bioss antibodies.bs-55207R), ULK1(1:1000,Zenbio, R381887), PINK1 (1:1000, Wanleibio, WL04963), Parkin (1:1000, Servicebi, GB11596),GAPDH (1:5000, Servicebio, GB15004) ,OPA1(1:1000,Proterntech, 27733-1-AP), Beclin-1(1:1000, Cell Signaling Technology, #3495) and Fis-1(1:1000, Cell Signaling Technology, #32525). After washing the membrane three times with TBST for ten minutes each time, it was incubated with goat anti-Rabbit IgG secondary antibody (1:10000, Proteintech, RGAR006) at room temperature for 1.5 h. Finally, after washing with TBST, protein expression was detected and analyzed using an Odyssey two-color infrared scanning fluorescence imaging system(LI-COR, Germany).

Statistical analysis

The experimental data were subjected to normality and homogeneity of variance tests using SPSS (Version 26) software. The results were presented as mean ± standard deviation. One-way ANOVA was employed for comparing experimental data following a normal distribution and met the assumptions of homogeneity of variance across multiple groups. For data not meeting the assumptions of normality or variance homogeneity, non-parametric tests were used to assess differences. GraphPad Prism 8 was utilized to generate plots. $P < 0.05$ was considered statistically significant.

Results

Astaxanthin prevents DOX-induced left ventricular dysfunction

On the 16th day of the study, echocardiography was performed on each rat to assess cardiac function. As illustrated in Fig. 1, the EF and FS of rats in the DOX group were significantly lower compared with those in the sham group ($P < 0.05$). Both doses of astaxanthin treatment resulted in a substantial increase in EF and FS compared to the DOX group. However, no significant difference was observed between the two ASTA groups.

Astaxanthin prevents DOX-induced myocardial damage

To evaluate the protective effect of astaxanthin against DOX-induced cardiac injury, rat serum cardiac troponin-I (cTn-I) levels were measured on the 16th day of the study. cTn-I is a specific marker of cardiomyocyte injury that reflects the degree of myocardial injury with higher specificity and sensitivity compared to traditional myocardial enzyme markers. Interestingly, cTn-I levels were significantly elevated in the DOX group, whilst astaxanthin treatment significantly reversed this increase ($P < 0.05$) (Fig. 2.A).

To investigate the impact of astaxanthin on rat cardiac histomorphological changes, routine HE staining (Fig. 2.B) was performed on rat cardiac tissue on the 16th day of the study. Under light microscopy, myocardial tissues in the sham group displayed clear structural integrity with uniformly colored fibers, well-defined cell boundaries, and no apparent pathological alterations. In the DOX group, occasional myocardial nuclear rupture, cytoplasm disintegration, and minimal lymphocyte infiltration were noted. Conversely, the ASTA-treated

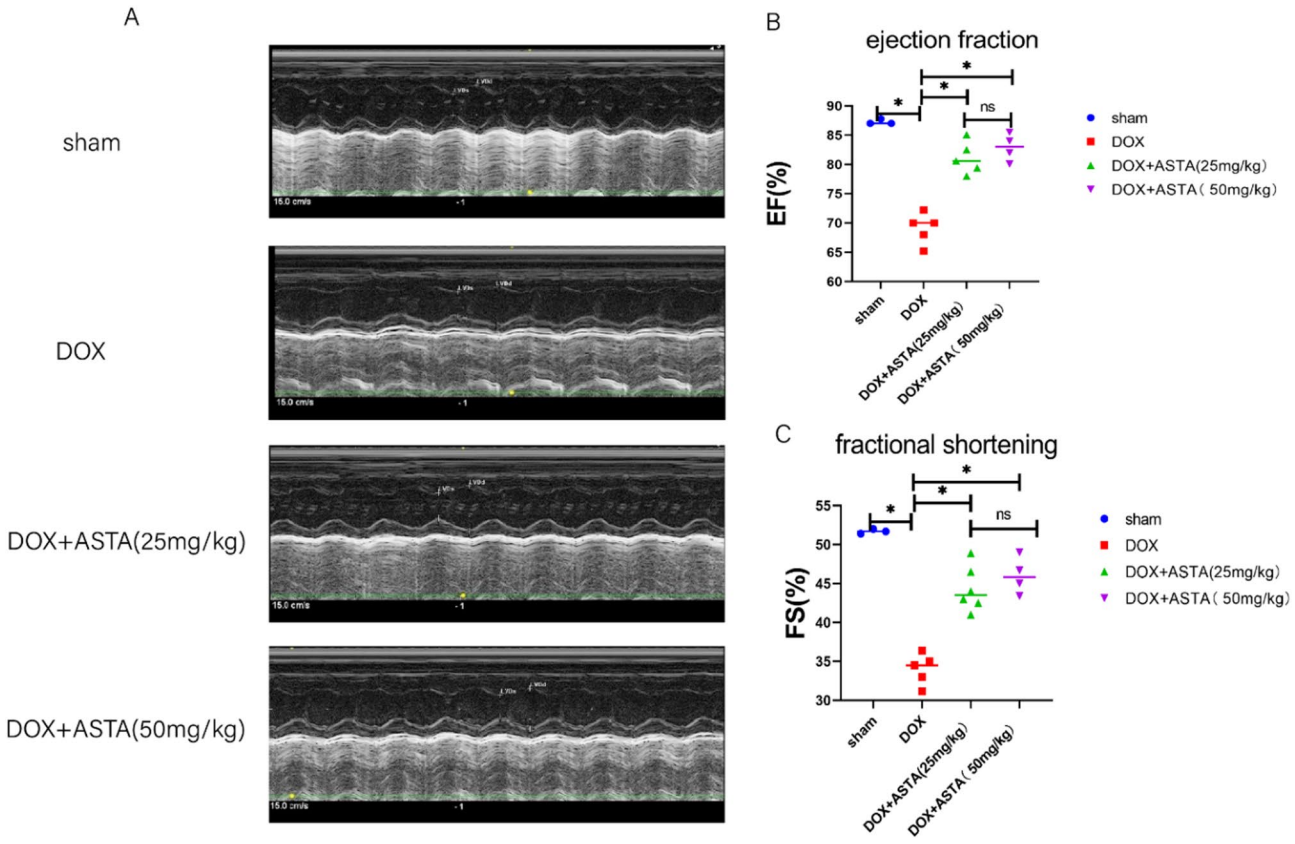

Fig. 1. ASTA can increase the left ventricular ejection fraction and left ventricular fractional shortening induced by DOX. (**A**) Representative M-ultrasound images in each group. (**B**) The results of EF in each group. Dox decreased the EF in rats, and ASTA treatment resulted in a statistically significant increase in EF compared to the DOX group. (**C**) The result of FS in each group. Dox decreased the FS in rats, and ASTA treatment resulted in a statistically significant increase in FS compared to the DOX group. Values are expressed as the mean ± standard deviation. Sham group: $n = 3$; other groups: $n = 6$ each. $^*P < 0.05$. ns: no significance. DOX: Doxorubicin; ASTA: Astaxanthin; EF: Ejection fraction; FS: Fractional shortening.

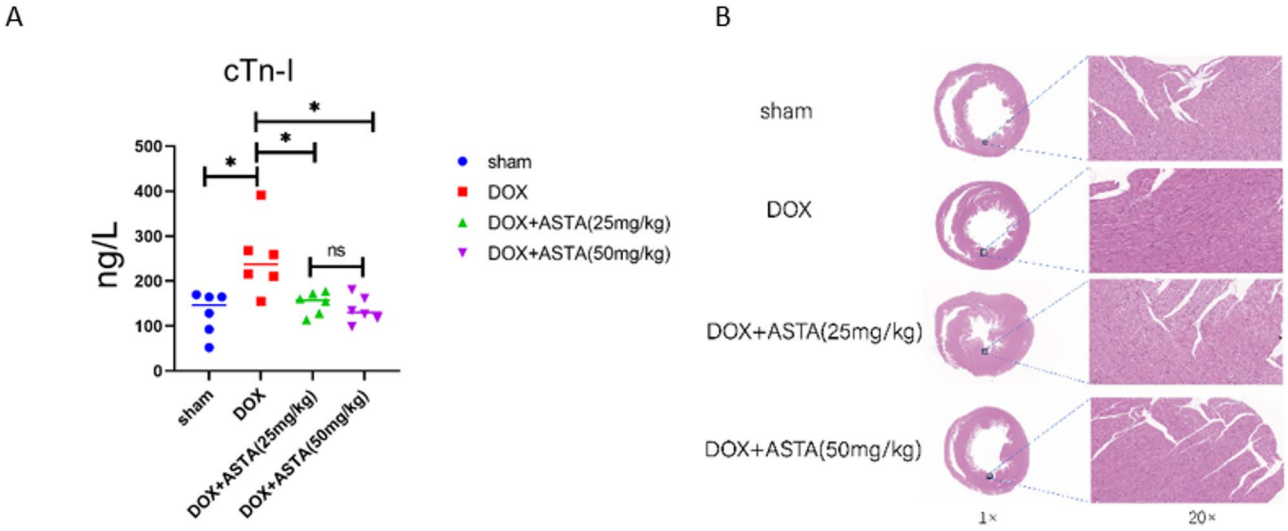

Fig. 2. Astaxanthin can attenuate myocardial injury induced by DOX. The above samples were collected on the 16th day of the study. (**A**) The serum levels of cTn-I in each group. The content of serum cTn-I in the DOX group increased. After treatment with ASTA, the content of serum cTn-I decreased. (**B**) HE staining of the hearts in each group. ASTA can alleviate the myocardial cell damage and immune cell infiltration resulting from doxorubicin. (left:1×, right:20×) Values are expressed as the mean ± standard deviation. $n = 6$. $^{*}P < 0.05$. ns: no significance. DOX: Doxorubicin; ASTA: Astaxanthin; Tn-I: troponin-I.

group displayed clear heart tissue structure with distinct cell boundaries and absence of noticeable necrosis or inflammatory cell infiltration.

Astaxanthin prevents cardiac mitochondrial structural and functional damage caused by DOX

The electron microscope serves as a crucial tool for observing the mitochondrial structure. To further expound on the protective effect of ASTA, transmission electron microscopy was utilized to examine the mitochondrial alterations of myocardial cells in each experimental group on the 16th day (Fig. 3A). In the sham group, cardiomyocytes appeared normal, with minimally swollen mitochondria and visible membranes and ridges. Conversely, cardiomyocytes in the DOX group displayed evident aberrations, characterized by moderate edema and an oval shape, with only a limited number of mitochondria retaining their structural ridges. Additionally, numerous vacuoles and autophagosomes were observed within the cytoplasm. The degree of myocardial cell damage was lower in both ASTA-treated group compared to the DOX groups. Specifically, mild mitochondrial edema and fewer autophagosomes were noted in both ASTA-treated group. Based on the assessment approach outlined by Li et al.[38]., the Flameng score is employed to assess mitochondrial damage (Fig. 3B). The specific scoring rules are detailed in Appendix 1. Mitochondria are the central site of energy metabolism within cells, and their primary function is to generate ATP. Therefore, the ATP levels in cells can directly reflect mitochondrial function. In our study, astaxanthin increased ATP content in rat cardiac tissue, indicating its ability to alleviate DOX-induced cardiac mitochondrial dysfunction (Fig. 3C).

Astaxanthin improves the imbalance in cardiac mitochondrial dynamics induced by DOX

Mitochondria are highly dynamic organelles that regulate their size and shape in response to various stress conditions through coordinated division, fusion, and transport functions. To further investigate the protective effect of astaxanthin against DOX-induced cardiac injury, we assessed the expression levels of DRP1, Mfn2,OPA1 and Fis-1 using western blot analysis (Fig. 4). In the DOX group, compared to the sham group, there was an increase in DRP1 and Fis-1 expression accompanied by a decrease in Mfn2 and OPA1 expression. However, after treatment with astaxanthin, there was a significant decrease in DRP1 and Fis-1 expression along with an increase in Mfn2 and OPA1 expression. These findings suggest that astaxanthin can ameliorate the imbalance of cardiac mitochondrial fusion and division induced by DOX.

Astaxanthin attenuates DOX-induced aberrant activation of cardiac mitochondrial autophagy through the PINK1/Parkin pathway

The results of TEM demonstrated mitochondrial autophagy played a pivotal role in doxorubicin-induced cardiac injury. To further examine the relationship between mitochondrial autophagy and the protective effect of astaxanthin, the expression levels of key proteins closely associated with mitochondrial autophagy, including Unc-51 Like Autophagy Activating Kinase 1 (ULK1), PTEN-Induced Putative Kinase 1 (PINK1), Parkin RBR E3 Ubiquitin Protein Ligase (Parkin), Beclin-1, Sequestosome 1(P62), and Microtubule-Associated Proteins 1 A/1B Light Chain 3 (LC3), were detected. As depicted in Fig. 5, compared to the sham group, the expression levels of ULK1, Parkin, Beclin-1 and LC3 were significantly higher in the DOX group, whereas those of P62

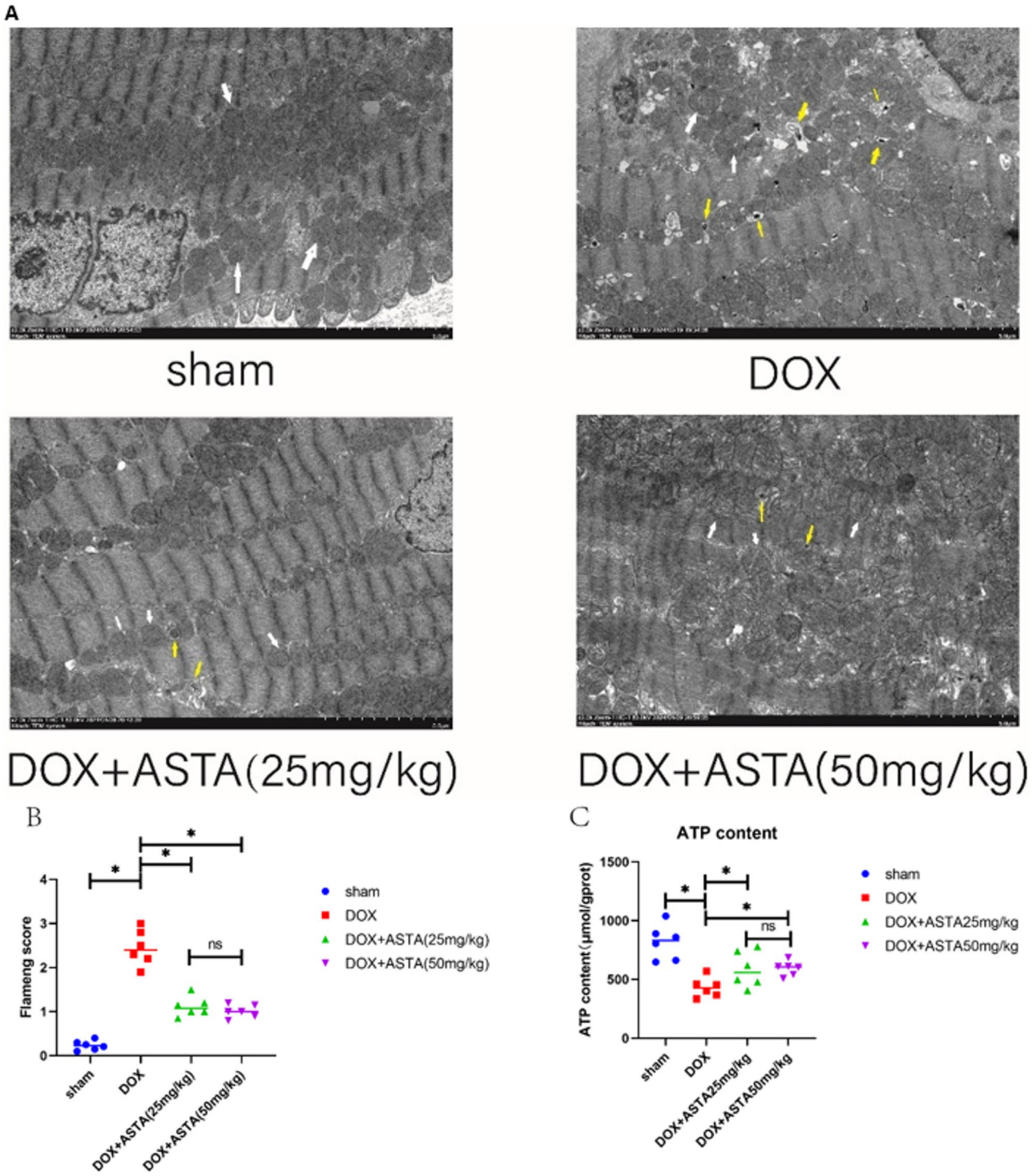

Fig. 3. Transmission electron microscopy images of myocardial cells in each group. The above samples were collected on the 16th day of the study. (**A**) Electron microscopy images of hearts in each group. ASTA mitigates cardiac mitochondrial edema and rupture mediated by doxorubicin and reduces the quantity of autophagosomes. The scale is 5.0 μm. The white arrow marks normal mitochondria, and the yellow arrow marks autophagosomes. (**B**) The results of the flameng scorce on mitochondria. A higher flameng score indicates more severe mitochondrial damage. ASTA effectively ameliorated cardiac mitochondrial damage induced by DOX. (**C**) The results indicate the ATP content in cardiomyocytes. Values are expressed as the mean ± standard deviation. $n = 6$. $^*P < 0.05$. ns: no significance, DOX: Doxorubicin, ASTA: Astaxanthin.

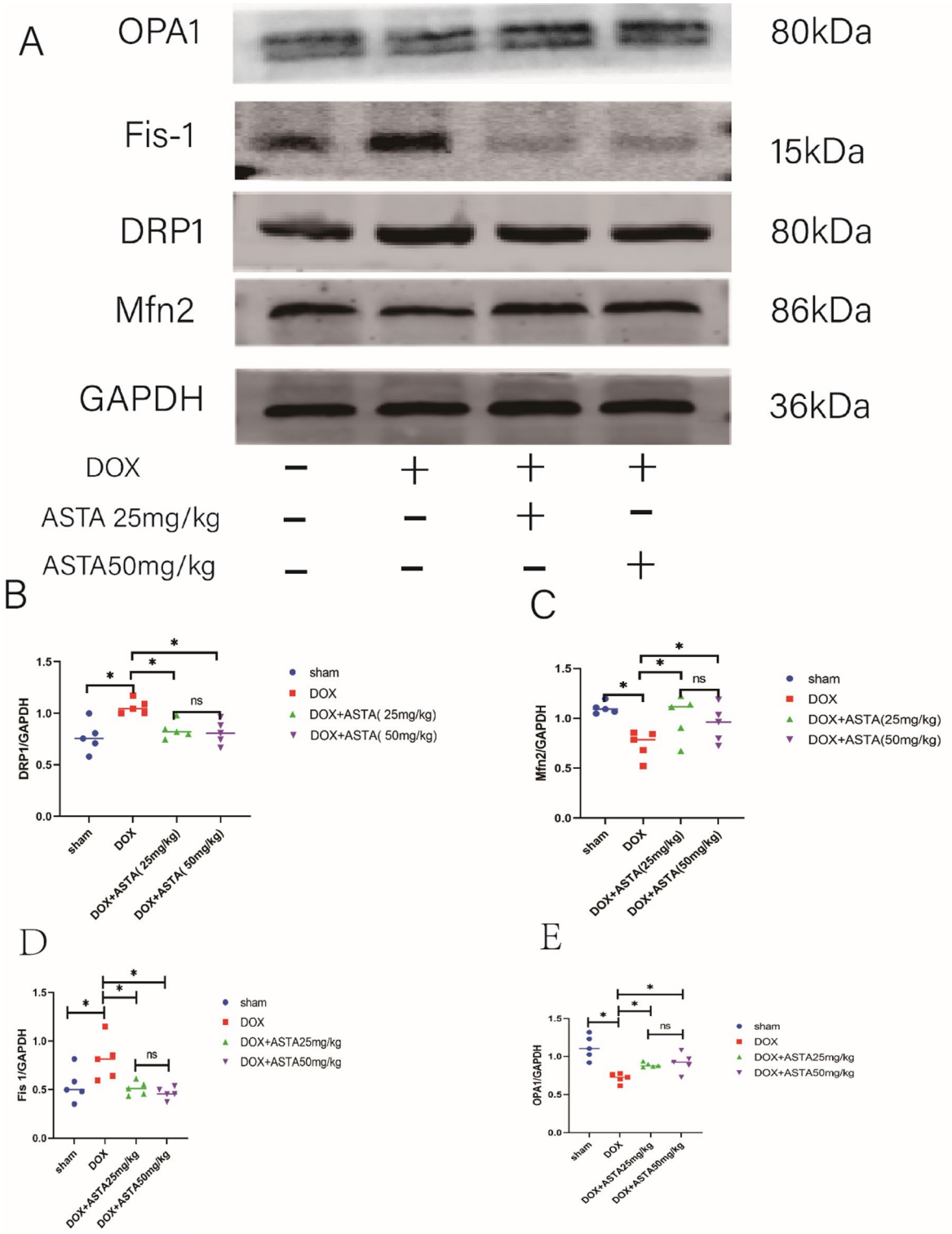

Fig. 4. ASTA can reduce the expression of DRP1 and Fis-1 and increase the expression of Mfn2 and OPA1 in DOX-induced cardiomyocytes. (**A**) Western blot (WB) stripes of DRP1,Mfn2, OPA1 and Fis-1. (**B**-**E**) **S**tatistical analysis of the WB strip of DRP1, Mfn 2, OPA1 and Fis-1. ASTA decreased the expression of DRP1 and Fis-1, inhibited cardiac excessive mitochondrial fission induced by DOX. And ASTA augmented the expression of Mfn2 and OPA1, facilitated cardiac mitochondrial fusion. The measurement data were presented as mean ± standard deviation. $n = 5$, $^*P < 0.05$. ns: no significance. DOX: Doxorubicin; ASTA: Astaxanthin; DRP1: Dynamin-related protein 1; Mfn2: Mitochondrial fusion protein 2. OPA1: Optic Atrophy 1; Fis-1:Fission 1 Protein.

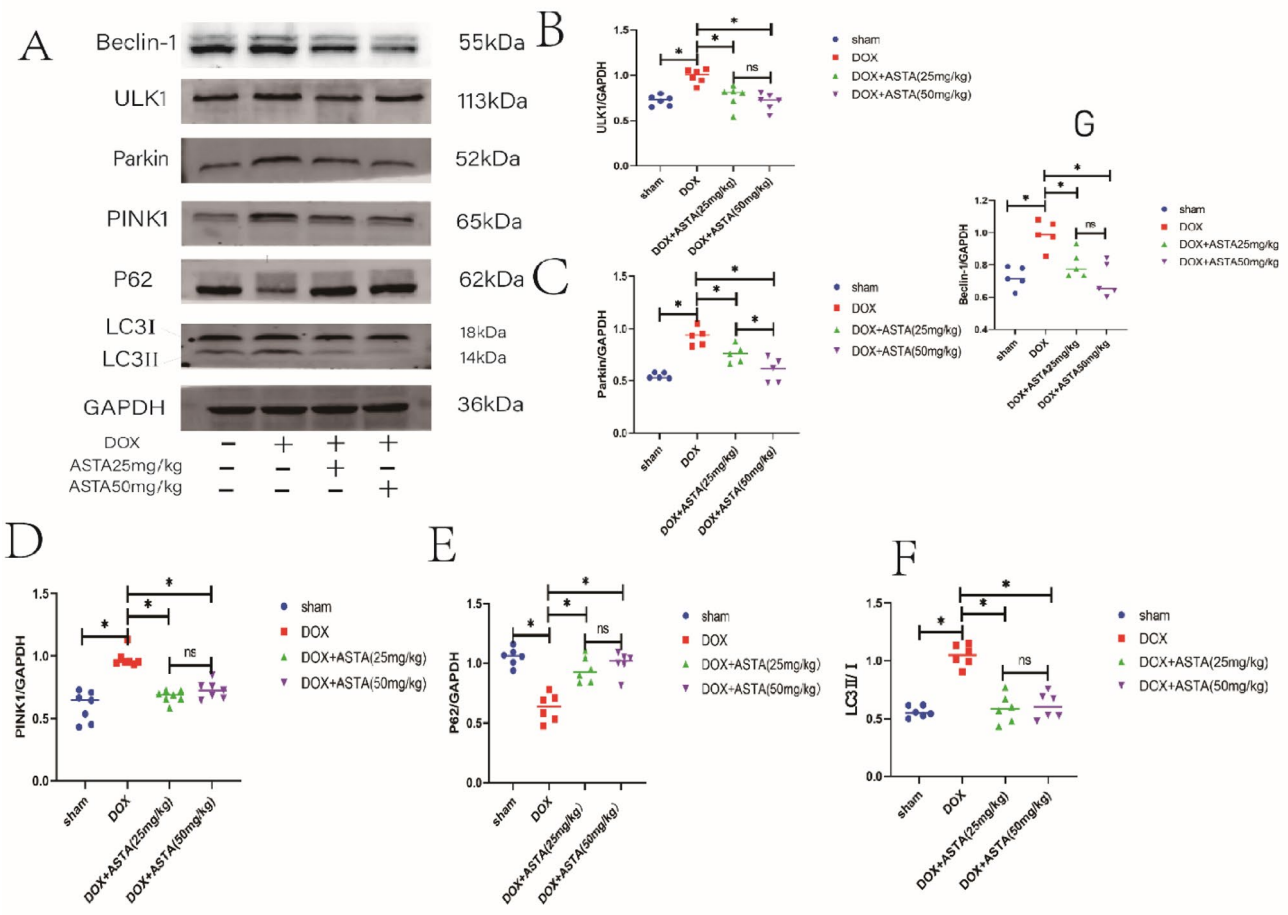

Fig. 5. Astaxanthin exhibits inhibitory effects on DOX-induced cardiac mitochondrial autophagy. (**A**) WB bands of mitochondrial autophagy-associated proteins ULK1, Parkin, Beclin-1,PINK1, P62, and LC3. (**B-G**) WB analysis data of ULK1, Parkin and PINK1, P62, LC3 and Beclin-1 were obtained. ASTA reduces the expression of ULK1, Parkin, Beclin-1and PINK1, lowers the ratio of LC3II to LC3I, and increases the expression of P62, suggesting that astaxanthin can alleviate cardiac mitochondrial autophagy induced by DOX. The measurement data were presented as mean ± standard deviation, $n = 6$, *P value < 0.05. ns: no significance. DOX: Doxorubicin; ASTA: Astaxanthin; ULK1: Unc-51 Like Autophagy Activating Kinase 1; PINK1: PTEN-Induced Putative Kinase 1; Parkin: Parkin RBR E3 Ubiquitin Protein Ligase; P62: Sequestosome 1; LC3: Microtubule-Associated Proteins 1 A/1B Light Chain 3.

were lower ($P < 0.05$), indicating an active state of mitochondrial autophagy. Compared to the DOX group, the expression levels of ULK1, Parkin, Beclin-1 and PINK1 were significantly lower in both ASTA groups ($P < 0.05$), accompanied by a lower LC3II/LC3I ratio ($P < 0.05$) and higher expression levels of P62 ($P < 0.05$), signaling that ASTA inhibited mitochondrial autophagy (Fig. 5).

Discussion

Currently, certain anticancer medications (e.g., anthracyclines such as DOX) frequently induce severe cardiac dysfunction while exerting their anti-tumorigenic effects[39]. Mitochondria are regarded as the primary target organelles of DOX-induced cardiac injury[12]. ASTA can penetrate into mitochondria in the cytoplasm[32]. In various cardiac diseases, ASTA can improve cardiac function by inhibiting mitochondrial swelling[40–42]. In the rat model of DOX-induced cardiac injury generated in this study, ASTA lowered serum cTn-I levels, thereby attenuating the decline in cardiac function induced by DOX, the imbalance in mitochondrial fusion and fission, and mitochondrial autophagy. We posit that ASTA mitigates DOX-induced cardiac mitochondrial damage and exerts cardioprotective effects by affecting mitochondrial dynamics and mitochondrial autophagy.

In order to detect cardiac damage induced by DOX, regular cardiac function monitoring is recommended. However, this method is associated with a delayed response[43]. Troponin is an early organ-specific biomarker for myocardial injury. Moreover, studies have identified cTn-I as a risk marker for a significant future reduction in LVEF[44]. More importantly, existing evidence suggests that patients treated with anthracycline drugs or trastuzumab have elevated cTn-I levels[45,46]. Furthermore, in the 2022 European Society of Cardiology clinical guidelines on cardio-oncology, cardiac troponin I is recommended for diagnosing anthracycline-induced

myocardial injury and guiding cardioprotective therapy[2]. Therefore, we propose that cTn-I may serve as a valuable marker for assessing the cardiotoxicity of DOX.

According to an earlier study, mitochondrial dysfunction is an early indicator of DOX-induced myocardial cell injury[47]. Mitochondria are crucial organelles responsible for cellular energy metabolism and adapt to cellular and environmental fluctuations through fusion and fission[12,27,48]. It is worthwhile emphasizing that their morphology is governed by fusion proteins and fission proteins. Studies have concluded that DOX decreases ΔΨm, thereby driving the opening of the mitochondrial Permeability Transition Pore (mPTP) and inhibiting cardiac mitochondrial fusion[48,49]. Mitochondrial function exhibits progressive impairment alongside increased mitochondrial fission[50]. In our study, the intracellular ATP content in the doxorubicin-treated group was significantly lower than in the Sham group. Notably, ASTA treatment effectively restored mitochondrial ATP content within cells. In rat hearts, DOX facilitates the phosphorylation of Drp1 at serine 616, which initiates mitochondrial fission[51]. Noteworthily, ASTA improves the respiratory control index, enhances mitochondrial fusion, and inhibits mitochondrial fission in the mitochondria in rat hearts after isoproterenol-induced injury[52]. Herein, DOX upregulated the expression of Drp1 and Fis-1, downregulated that of Mfn2 and OPA1, shifting the mitochondrial dynamic balance towards fission. On the other hand, ASTA treatment inhibited mitochondrial fission by down-regulating the expression of DRP1 and Fis-1, up-regulating that of Mfn2 and OPA1, thereby restoring mitochondrial fusion. This indicates that in the DOX-induced cardiac injury model, ASTA alleviates cardiac mitochondrial damage by inhibiting mitochondrial fission and promoting mitochondrial fusion.

After fission via Drp1, the fate of fragmented mitochondria is contingent upon their capacity to restore mitochondrial membrane potential; healthy mitochondria can restore mitochondrial membrane potential and re-engage in the fusion-fission cycle, while those unable to recover are marked and eliminated via mitophagy[53,54]. Mitochondrial autophagy is a ubiquitous mitochondrial self-renewal mechanism in eukaryotic cells[55]. To sustain physiological activities, mitochondria eliminate damaged mitochondria via the mitophagy pathway[56]. Previous studies indicated that heightened levels of mitochondrial autophagy exacerbate mitochondrial damage and compromise overall mitochondrial function in DOX-induced cardiomyocyte injury[57,58]. Consistent with the observations of earlier studies, this study unveiled the presence of numerous scattered autophagosomes in the DOX group. The results of western blot analysis uncovered an elevated Beclin-1 and LC3-II/LC3-I ratio, down-regulated p62 expression, suggesting that DOX activated mitochondrial autophagy and disrupted mitochondrial function. However, studies investigating the role of mitochondrial autophagy in DOX-induced cardiomyocyte injury have yielded conflicting findings. Some studies pointed out that increased mitochondrial autophagy facilitates mitochondrial rejuvenation, thereby preserving mitochondrial function in Dox-induced cardiotoxicity[59,60]. This controversial perspective may arise from variations in dosage, duration, and drug interactions[61]. In the present study, treatment with ASTA decreased the Beclin-1 and LC3-II/LC3-I ratio, up-regulated the expression of p62, indicating inhibition of autophagy. These results suggest that ASTA can alleviate doxorubicin-induced cardiac mitochondrial damage by suppressing mitochondrial autophagy, thereby protecting cardiac function. Some studies indicated that ASTA can suppress autophagy and concomitantly enhance mitochondrial function, in line with the results of this study[29,62].

Mitophagy typically occurs through two pathways, namely the ubiquitin-dependent pathway and the ubiquitin-independent pathway[63]. Among them, mitophagy mediated by the PINK1/Parkin pathway is the most extensively investigated. Under physiological conditions, PINK1 is degraded at the inner mitochondrial membrane, whilst Parkin remains in an inactive state[64]. Nevertheless, following ΔΨm disruptions, the channel for PINK1 to enter the inner mitochondrial membrane is obstructed, resulting in its accumulation on the outer mitochondrial membrane[65]. On the outer mitochondrial membrane, PINK1 and Parkin interact to ubiquitinate proteins at the outer mitochondrial membrane[66,67]. The accumulation of these ubiquitinated proteins contributes to the recruitment of the autophagy initiation factor ULK1, thereby stimulating mitophagy[66]. DOX-induced mitophagy and mitochondrial damage in cardiomyocytes are partially mediated by the dysregulation of the PINK1/parkin pathway[61]. Studies have exposed that the administration of ASTA can confer protective effects by regulating mitochondrial autophagy and the PINK1/Parkin pathway[68]. Herein, the expression levels of the PINK and Parkin proteins were significantly increased in the DOX group, suggesting that DOX activates mitochondrial autophagy by mediating the PINK1/parkin pathway. After treatment with ASTA, the expression levels of the PINK and Parkin proteins decreased, indicating that astaxanthin exerted cardioprotective effects by regulating mitochondrial autophagy via the PINK1/Parkin pathway in DOX-induced cardiac injury.

Astaxanthin not only has demonstrated therapeutic potential in doxorubicin-induced cardiac injury, but also has shown efficacy in various cancer types, including neuroblastoma, breast cancer and gastrointestinal cancer, through its ability to induce apoptosis, inhibit metastasis and disrupt cell growth[69–71]. Glioblastoma is one of the most aggressive primary brain cancers, with a very low survival rate[72]. Researchers found that when pretreating two human GBM cell lines, U251-MG and T98-MG, with ASTA, their sensitivity to tumor necrosis factor-related apoptosis-inducing ligand (TRAIL) was significantly enhanced, thereby increasing the apoptotic response[69]. In addition, Shao et al. demonstrated that AXT inhibits the proliferation of H22 liver cancer cells both in vitro and in vivo, and induces apoptosis and necrosis of the cells[73]. Moreover, ASTA treatment can reduce the ROS level in HepG2 cells, thereby significantly inhibiting cell growth. Notably, this cytotoxicity is selective, that is, it does not cause damage to normal liver cells (THLE-2 cells), highlighting the potential of ASTA for targeted cancer therapy without harming healthy cells[74]. As a common health care products, astaxanthin, when used in combination with doxorubicin during chemotherapy, may not only alleviate the cardiotoxicity caused by doxorubicin but also assist doxorubicin in exerting its anti-tumor effect, providing a laboratory basis for the treatment of doxorubicin-induced cardiac injury.

In our research, we established a rat model of DOX-induced cardiac injury and observed whether ASTA improves DOX-induced cardiac mitochondrial damage and exerts cardioprotective effects by affecting mitochondrial dynamics and autophagy. Several limitations exist in our current research. The research was

limited to investigate astaxanthin's protective effects against doxorubicin-induced cardiac injury at the animal model level, and did not extend to explore its underlying mechanisms through in vitro experimental.

Conclusion

In summary, ASTA ameliorated myocardial damage and cardiac dysfunction in a rat model of DOX-induced cardiac injury. The potential mechanism may involve ASTA down-regulating the expression of DRP1 and Fis-1 and up-regulating that of Mfn2 and OPA1 to induce mitochondrial fusion, limit mitochondrial fission, and suppress mitochondrial autophagy mediated by the PINK1/Parkin pathway.

Data availability

The datasets generated during and analyzed during the current study are available from the corresponding author upon reasonable request.

Received: 27 April 2025; Accepted: 22 August 2025
Published online: 01 September 2025

References

1. Christidi, E. & Brunham, L. R. Regulated cell death pathways in doxorubicin-induced cardiotoxicity. *Cell Death Dis.* **12**, 339. https://doi.org/10.1038/s41419-021-03614-x (2021).
2. Lyon, A. R. et al. 2022 ESC guidelines on cardio-oncology developed in collaboration with the European hematology association (EHA), the European society for therapeutic radiology and oncology (ESTRO) and the international Cardio-Oncology society (IC-OS). *Eur. Heart J.* **43**, 4229–4361. https://doi.org/10.1093/eurheartj/ehac244 (2022).
3. Meiners, B., Shenoy, C. & Zordoky, B. N. Clinical and preclinical evidence of sex-related differences in anthracycline-induced cardiotoxicity. *Biology Sex. Differences*. **9** https://doi.org/10.1186/s13293-018-0198-2 (2018).
4. Lai, Y. et al. Non-invasive transcutaneous vagal nerve stimulation improves myocardial performance in doxorubicin-induced cardiotoxicity. *Cardiovascular. Res.* **118**, 1821–1834. https://doi.org/10.1093/cvr/cvab209 (2022).
5. Kolaric, K. et al. A phase II trial of cardioprotection with cardioxane (ICRF-187) in patients with advanced breast cancer receiving 5-fluorouracil, doxorubicin and cyclophosphamide. *Oncology* **52**, 251–255. https://doi.org/10.1159/000227467 (1995).
6. Swain, S. M. et al. Cardioprotection with Dexrazoxane for doxorubicin-containing therapy in advanced breast cancer. *J. Clin. Oncology: Official J. Am. Soc. Clin. Oncol.* **15**, 1318–1332. https://doi.org/10.1200/jco.1997.15.4.1318 (1997).
7. Rabelo, E. et al. Baroreflex sensitivity and oxidative stress in adriamycin-induced heart failure. *Hypertens. (Dallas Tex. : 1979)*. **38**, 576–580. https://doi.org/10.1161/hy09t1.096185 (2001).
8. Wattanapitayakul, S. K. et al. Screening of antioxidants from medicinal plants for cardioprotective effect against doxorubicin toxicity. *Basic Clin. Pharmacol. Toxicol.* **96**, 80–87. https://doi.org/10.1111/j.1742-7843.2005.pto960112.x (2005).
9. Chaiswing, L. et al. Oxidative damage precedes nitrative damage in adriamycin-induced cardiac mitochondrial injury. *Toxicol. Pathol.* **32**, 536–547. https://doi.org/10.1080/01926230490502601 (2004).
10. Gilleron, M. et al. NADPH oxidases participate to doxorubicin-induced cardiac myocyte apoptosis. *Biochem. Biophys. Res. Commun.* **388**, 727–731. https://doi.org/10.1016/j.bbrc.2009.08.085 (2009).
11. Ascensão, A. et al. Acute exercise protects against calcium-induced cardiac mitochondrial permeability transition pore opening in doxorubicin-treated rats. *Clin. Sci. (London England: 1979)*. **120**, 37–49. https://doi.org/10.1042/cs20100254 (2011).
12. Wu, B. B., Leung, K. T. & Poon, E. N. Mitochondrial-Targeted therapy for Doxorubicin-Induced cardiotoxicity. *Int. J. Mol. Sci.* **23** https://doi.org/10.3390/ijms23031912 (2022).
13. Zhou, H., Ren, J., Toan, S. & Mui, D. Role of mitochondrial quality surveillance in myocardial infarction: from bench to bedside. *Ageing Res. Rev.* **66**, 101250. https://doi.org/10.1016/j.arr.2020.101250 (2021).
14. Wang, B. et al. AMPKα2 protects against the development of heart failure by enhancing mitophagy via PINK1 phosphorylation. *Circul. Res.* **122**, 712–729. https://doi.org/10.1161/circresaha.117.312317 (2018).
15. Huang, J. et al. Understanding anthracycline cardiotoxicity from mitochondrial aspect. *Front. Pharmacol.* **13** https://doi.org/10.3389/fphar.2022.811406 (2022).
16. Osataphan, N., Phrommintikul, A., Chattipakorn, S. C. & Chattipakorn, N. Effects of doxorubicin-induced cardiotoxicity on cardiac mitochondrial dynamics and mitochondrial function: insights for future interventions. *J. Cell. Mol. Med.* **24**, 6534–6557. https://doi.org/10.1111/jcmm.15305 (2020).
17. Forte, M. et al. The role of mitochondrial dynamics in cardiovascular diseases. *Br. J. Pharmacol.* **178**, 2060–2076. https://doi.org/10.1111/bph.15068 (2021).
18. Ding, M. et al. Mfn2-mediated mitochondrial fusion alleviates doxorubicin-induced cardiotoxicity with enhancing its anticancer activity through metabolic switch. *Redox Biol.* **52**, 102311. https://doi.org/10.1016/j.redox.2022.102311 (2022).
19. Catanzaro, M. P. et al. Doxorubicin-induced cardiomyocyte death is mediated by unchecked mitochondrial fission and mitophagy. *FASEB Journal: Official Publication Federation Am. Soc. Experimental Biology*. **33**, 11096–11108. https://doi.org/10.1096/fj.201802663R (2019).
20. Xu, Z. M., Li, C. B., Liu, Q. L., Li, P. & Yang, H. Ginsenoside Rg1 prevents Doxorubicin-Induced cardiotoxicity through the Inhibition of autophagy and Endoplasmic reticulum stress in mice. *Int. J. Mol. Sci.* **19** https://doi.org/10.3390/ijms19113658 (2018).
21. Lacombe, A. & Scorrano, L. The interplay between mitochondrial dynamics and autophagy: from a key homeostatic mechanism to a driver of pathology. *Semin. Cell Dev. Biol.* **161–162**, 1–19. https://doi.org/10.1016/j.semcdb.2024.02.001 (2024).
22. Xian, H. & Liou, Y. C. Functions of outer mitochondrial membrane proteins: mediating the crosstalk between mitochondrial dynamics and mitophagy. *Cell Death Differ.* **28**, 827–842. https://doi.org/10.1038/s41418-020-00657-z (2021).
23. Wang, X. et al. Ghrelin inhibits doxorubicin cardiotoxicity by inhibiting excessive autophagy through AMPK and p38-MAPK. *Biochem. Pharmacol.* **88**, 334–350. https://doi.org/10.1016/j.bcp.2014.01.040 (2014).
24. Kobayashi, S. et al. Transcription factor GATA4 inhibits doxorubicin-induced autophagy and cardiomyocyte death. *J. Biol. Chem.* **285**, 793–804. https://doi.org/10.1074/jbc.M109.070037 (2010).
25. Ajoolabady, A., Aslkhodapasandhokmabad, H., Aghanejad, A., Zhang, Y. & Ren, J. Mitophagy receptors and mediators: therapeutic targets in the management of cardiovascular ageing. *Ageing Res. Rev.* **62**, 101129. https://doi.org/10.1016/j.arr.2020.101129 (2020).
26. Chang, M. X. & Xiong, F. Astaxanthin and its effects in inflammatory responses and Inflammation-Associated diseases: recent advances and future directions. *Molecules (Basel Switzerland)*. **25** https://doi.org/10.3390/molecules25225342 (2020).
27. Krestinina, O., Baburina, Y. & Krestinin, R. Mitochondrion as a target of Astaxanthin therapy in heart failure. *Int. J. Mol. Sci.* **22** https://doi.org/10.3390/ijms22157964 (2021).
28. Pongkan, W. et al. β-Cryptoxanthin exerts greater cardioprotective effects on cardiac ischemia-reperfusion injury than Astaxanthin by attenuating mitochondrial dysfunction in mice. *Mol. Nutr. Food Res.* **61** https://doi.org/10.1002/mnfr.201601077 (2017).

29. Cai, X. et al. Astaxanthin activated the Nrf2/HO-1 pathway to enhance autophagy and inhibit ferroptosis, ameliorating Acetaminophen-Induced liver injury. *ACS Appl. Mater. Interfaces*. **14**, 42887–42903. https://doi.org/10.1021/acsami.2c10506 (2022).
30. Zou, Y. et al. Protective effects of Astaxanthin on Ochratoxin A-Induced liver injury: effects of Endoplasmic reticulum stress and mitochondrial Fission-Fusion balance. *Toxins* **16** https://doi.org/10.3390/toxins16020068 (2024).
31. Zhang, J. et al. Astaxanthin prevents pulmonary fibrosis by promoting myofibroblast apoptosis dependent on Drp1-mediated mitochondrial fission. *J. Cell. Mol. Med.* **19**, 2215–2231. https://doi.org/10.1111/jcmm.12609 (2015).
32. Duan, F., Li, H. & Lu, H. In vivo and molecular Docking studies of the pathological mechanism underlying adriamycin cardiotoxicity. *Ecotoxicol. Environ. Saf.* **256**, 114778. https://doi.org/10.1016/j.ecoenv.2023.114778 (2023).
33. Sawicki, K. T. et al. Preventing and treating anthracycline cardiotoxicity: new insights. *Annu. Rev. Pharmacol. Toxicol.* **61**, 309–332. https://doi.org/10.1146/annurev-pharmtox-030620-104842 (2021).
34. O'Connell, J. L. et al. Short-term and long-term models of doxorubicin-induced cardiomyopathy in rats: A comparison of functional and histopathological changes. *Experimental Toxicologic Pathology: Official J. Gesellschaft Fur Toxikologische Pathologie*. **69**, 213–219. https://doi.org/10.1016/j.etp.2017.01.004 (2017).
35. Kharin, S. N., Krandycheva, V. V., Strelkova, M. V., Tsvetkova, A. S. & Shmakov, D. N. Doxorubicin-induced changes of ventricular repolarization heterogeneity: results of a chronic rat study. *Cardiovasc. Toxicol.* **12**, 312–317. https://doi.org/10.1007/s12012-012-9172-0 (2012).
36. Alam, M. N. et al. Astaxanthin prevented oxidative stress in heart and kidneys of Isoproterenol-Administered aged rats. *J. Diet. Supplements*. **15**, 42–54. https://doi.org/10.1080/19390211.2017.1321078 (2018).
37. Boshra, S. A. & Astaxanthin Attenuates Adiponectin Calprotectin, miRNA222 and miRNA378 in obesity induced by High-Fat diet in rats. *Curr. Pharm. Biotechnol.* **23**, 609–618. https://doi.org/10.2174/1389201022666210810105804 (2022).
38. Li, L. et al. Polydatin prevents the induction of secondary brain injury after traumatic brain injury by protecting neuronal mitochondria. *Neural Regeneration Res.* **14**, 1573–1582. https://doi.org/10.4103/1673-5374.255972 (2019).
39. Cardinale, D. et al. Early detection of anthracycline cardiotoxicity and improvement with heart failure therapy. *Circulation* **131**, 1981–1988. https://doi.org/10.1161/circulationaha.114.013777 (2015).
40. Krestinin, R., Kobyakova, M., Baburina, Y., Sotnikova, L. & Krestinina, O. Astaxanthin protects against H(2)O(2)- and Doxorubicin-Induced cardiotoxicity in H9c2 rat myocardial cells. *Life (Basel Switzerland)*. **14** https://doi.org/10.3390/life14111409 (2024).
41. Fu, J. et al. Astaxanthin alleviates spinal cord ischemia-reperfusion injury via activation of PI3K/Akt/GSK-3β pathway in rats. *J. Orthop. Surg, Res.* **15**, 275. https://doi.org/10.1186/s13018-020-01790-8 (2020).
42. Mohammadi, S. G. et al. The effect of Astaxanthin supplementation on inflammatory markers, oxidative stress indices, lipid profile, uric acid level, blood pressure, endothelial function, quality of life, and disease symptoms in heart failure subjects. *Trials* **25**, 518. https://doi.org/10.1186/s13063-024-08339-8 (2024).
43. Inoue, K. et al. Early detection and prediction of Anthracycline-Induced Cardiotoxicity - A prospective cohort study. *Circulation Journal: Official J. Japanese Circulation Soc.* **88**, 751–759. https://doi.org/10.1253/circj.CJ-24-0065 (2024).
44. Cardinale, D. et al. Myocardial injury revealed by plasma troponin I in breast cancer treated with high-dose chemotherapy. *Annals Oncology: Official J. Eur. Soc. Med. Oncol.* **13**, 710–715. https://doi.org/10.1093/annonc/mdf170 (2002).
45. Ky, B. et al. Early increases in multiple biomarkers predict subsequent cardiotoxicity in patients with breast cancer treated with doxorubicin, taxanes, and trastuzumab. *J. Am. Coll. Cardiol.* **63**, 809–816. https://doi.org/10.1016/j.jacc.2013.10.061 (2014).
46. Mokuyasu, S., Suzuki, Y., Kawahara, E., Seto, T. & Tokuda, Y. High-sensitivity cardiac troponin I detection for 2 types of drug-induced cardiotoxicity in patients with breast cancer. *Breast Cancer (Tokyo Japan)*. **22**, 563–569. https://doi.org/10.1007/s12282-014-0520-8 (2015).
47. Green, P. S. & Leeuwenburgh, C. Mitochondrial dysfunction is an early indicator of doxorubicin-induced apoptosis. *Biochim. Biophys. Acta*. **1588**, 94–101. https://doi.org/10.1016/s0925-4439(02)00144-8 (2002).
48. Wu, L., Wang, L., Du, Y., Zhang, Y. & Ren, J. Mitochondrial quality control mechanisms as therapeutic targets in doxorubicin-induced cardiotoxicity. *Trends Pharmacol. Sci.* **44**, 34–49. https://doi.org/10.1016/j.tips.2022.10.003 (2023).
49. Krestinin, R. et al. The effect of Astaxanthin on mitochondrial dynamics in rat heart mitochondria under ISO-Induced injury. *Antioxid. (Basel Switzerland)*. **12** https://doi.org/10.3390/antiox12061247 (2023).
50. Jin, J. Y., Wei, X. X., Zhi, X. L., Wang, X. H. & Meng, D. Drp1-dependent mitochondrial fission in cardiovascular disease. *Acta Pharmacol. Sin.* **42**, 655–664. https://doi.org/10.1038/s41401-020-00518-y (2021).
51. Xia, Y. et al. LCZ696 improves cardiac function via alleviating Drp1-mediated mitochondrial dysfunction in mice with doxorubicin-induced dilated cardiomyopathy. *J. Mol. Cell. Cardiol.* **108**, 138–148. https://doi.org/10.1016/j.yjmcc.2017.06.003 (2017).
52. Kleele, T. et al. Distinct fission signatures predict mitochondrial degradation or biogenesis. *Nature* **593**, 435–439. https://doi.org/10.1038/s41586-021-03510-6 (2021).
53. Shirakabe, A. et al. Drp1-Dependent mitochondrial autophagy plays a protective role against pressure Overload-Induced mitochondrial dysfunction and heart failure. *Circulation* **133**, 1249–1263. https://doi.org/10.1161/circulationaha.115.020502 (2016).
54. Li, Y. et al. Increased Drp1 promotes autophagy and ESCC progression by MtDNA stress mediated cGAS-STING pathway. *J. Experimental Clin. Cancer Research: CR*. **41**, 76. https://doi.org/10.1186/s13046-022-02262-z (2022).
55. Goodall, E. A., Kraus, F. & Harper, J. W. Mechanisms underlying ubiquitin-driven selective mitochondrial and bacterial autophagy. *Mol. Cell.* **82**, 1501–1513. https://doi.org/10.1016/j.molcel.2022.03.012 (2022).
56. Nguyen, T. N., Padman, B. S. & Lazarou, M. Deciphering the molecular signals of PINK1/Parkin mitophagy. *Trends Cell Biol.* **26**, 733–744. https://doi.org/10.1016/j.tcb.2016.05.008 (2016).
57. Zhou, J. et al. Sphingosylphosphorylcholine ameliorates doxorubicin-induced cardiotoxicity in zebrafish and H9c2 cells by reducing excessive mitophagy and mitochondrial dysfunction. *Toxicol. Appl. Pharmcol.* **452**, 116207. https://doi.org/10.1016/j.taap.2022.116207 (2022).
58. Lu, L. et al. Follistatin-like protein 1 attenuates doxorubicin-induced cardiomyopathy by inhibiting MsrB2-mediated mitophagy. *Mol. Cell. Biochem.* **479**, 1817–1831. https://doi.org/10.1007/s11010-024-04955-9 (2024).
59. Xiao, D. et al. Enhanced mitophagy mediated by the yap/parkin pathway protects against DOX-induced cardiotoxicity. *Toxicol. Lett.* **330**, 96–107. https://doi.org/10.1016/j.toxlet.2020.05.015 (2020).
60. Wang, P. et al. SESN2 protects against doxorubicin-induced cardiomyopathy via rescuing mitophagy and improving mitochondrial function. *J. Mol. Cell. Cardiol.* **133**, 125–137. https://doi.org/10.1016/j.yjmcc.2019.06.005 (2019).
61. Yin, J. et al. Doxorubicin-induced mitophagy and mitochondrial damage is associated with dysregulation of the PINK1/parkin pathway. *Toxicol. Vitro: Int. J. Published Association BIBRA*. **51**, 1–10. https://doi.org/10.1016/j.tiv.2018.05.001 (2018).
62. Wang, X. et al. Docosahexaenoic Acid-Acylated Astaxanthin monoester ameliorates Amyloid-β pathology and neuronal damage by restoring autophagy in alzheimer's disease models. *Mol. Nutr. Food Res.* **68**, e2300414. https://doi.org/10.1002/mnfr.202300414 (2024).
63. Han, S., Zhang, M., Jeong, Y. Y., Margolis, D. J. & Cai, Q. The role of mitophagy in the regulation of mitochondrial energetic status in neurons. *Autophagy* **17**, 4182–4201. https://doi.org/10.1080/15548627.2021.1907167 (2021).
64. Pickrell, A. M. & Youle, R. J. The roles of PINK1, parkin, and mitochondrial fidelity in parkinson's disease. *Neuron* **85**, 257–273. https://doi.org/10.1016/j.neuron.2014.12.007 (2015).
65. Ham, S. J. et al. PINK1 and parkin regulate IP(3)R-mediated ER calcium release. *Nat. Commun.* **14**, 5202. https://doi.org/10.1038/s41467-023-40929-z (2023).

66. Geisler, S. et al. PINK1/Parkin-mediated mitophagy is dependent on VDAC1 and p62/SQSTM1. *Nat. Cell Biol.* **12**, 119–131. https://doi.org/10.1038/ncb2012 (2010).
67. Quinn, P. M. J., Moreira, P. I., Ambrósio, A. F. & Alves, C. H. PINK1/PARKIN signalling in neurodegeneration and neuroinflammation. *Acta Neuropathol. Commun.* **8**, 189. https://doi.org/10.1186/s40478-020-01062-w (2020).
68. Yamamoto, A., Sly, P. D., Begum, N., Yeo, A. J. & Fantino, E. Resveratrol and Astaxanthin protect primary human nasal epithelial cells cultured at an Air-liquid interface from an acute oxidant exposure. *J. Cell. Signal.* **3**, 207–217. https://doi.org/10.33696/signaling.3.084 (2022).
69. Shin, J., Nile, A., Saini, R. K. & Oh, J. W. Astaxanthin sensitizes low SOD2-Expressing GBM cell lines to TRAIL treatment via pathway involving mitochondrial membrane depolarization. *Antioxid. (Basel Switzerland)*. **11** https://doi.org/10.3390/antiox11020375 (2022).
70. Kim, M. S., Ahn, Y. T., Lee, C. W., Kim, H. & An, W. G. Astaxanthin modulates apoptotic molecules to induce death of SKBR3 breast cancer cells. *Mar. Drugs*. **18** https://doi.org/10.3390/md18050266 (2020).
71. Yadav, K. et al. Comparing Pharmacological potential of freshwater microalgae carotenoids towards antioxidant and Anti-proliferative activity on liver cancer (HUH7) cell line. *Appl. Biochem. Biotechnol.* **196**, 2053–2066. https://doi.org/10.1007/s12010-023-04635-2 (2024).
72. Ostrom, Q. T. et al. CBTRUS Statistical Report: Primary Brain and Other Central Nervous System Tumors Diagnosed in the United States in 2013–2017. *Neuro-oncology* 22, iv1-iv96, (2020). https://doi.org/10.1093/neuonc/noaa200
73. Shao, Y. et al. Astaxanthin inhibits proliferation and induces apoptosis and cell cycle arrest of mice H22 hepatoma cells. *Med. Sci. Monitor: Int. Med. J. Experimental Clin. Res.* **22**, 2152–2160. https://doi.org/10.12659/msm.899419 (2016).
74. Zhang, X., Li, W., Dou, X., Nan, D. & He, G. Astaxanthin encapsulated in biodegradable calcium alginate microspheres for the treatment of hepatocellular carcinoma in vitro. *Appl. Biochem. Biotechnol.* **191**, 511–527. https://doi.org/10.1007/s12010-019-03174-z (2020).

Acknowledgements

The present study was supported by the Guangxi Natural Science Foundation (No. 2024GXNSFBA010292) and 2020 Guangxi University Young and Middle-aged Teachers' Basic Research Ability Improvement Project (No. 2020KY03032).

Author contributions

H.Y.J and W.D.: Methodology, Validation, Investigation, Formal analysis, Writing the original draft. W.Q.Q. and H.S.S.: Conceptualization, Formal analysis. Z.Y.S. and D.J.Q. and C.J.Y.: Methodology. X.L. and Z.J.H.: Writing review & editing, Conceptualization, Supervision, Project administration, Funding acquisition. All authors read and approved the final manuscript.

Funding

The present study was supported by the Guangxi Natural Science Foundation (No.2024GXNSFBA010292) and the 2020 Guangxi University Young and Middle-aged Teachers' Basic Research Ability Improvement Project (No.2020KY03032).

Declarations

Ethics approval and consent to participate

The protocol was approved by the Animal Ethics Committee of Guangxi Medical University, and all animal procedures were performed in accordance with the "Guiding Principles for the Care and Use of Animals in the Field of Physiological Sciences" (protocol code 202404007, 2024.04.07). All experiments were conducted in accordance with ARRIVE guidelines. In the animal experiments described in this manuscript, all authors have confirmed the animal experimental protocols involved in this study. These experiments were conducted under the oversight of the Ethics Committee of Guangxi Medical University.

Consent for publication

All the authors have approved the manuscript and agree with submission to your esteemed journal.

Competing interests

The authors declare no competing interests.

Additional information

Supplementary Information The online version contains supplementary material available at https://doi.org/10.1038/s41598-025-17253-1.

Correspondence and requests for materials should be addressed to L.x. or J.Z.